BIOCHEMISTRY
including biophysical chemistry & molecular biology

Article

pubs.acs.org/biochemistry

Structural Dynamics of a Mitochondrial tRNA Possessing Weak Thermodynamic Stability

Hari Bhaskaran,[†,‡,∥] Takaaki Taniguchi,[§] Takeo Suzuki,[§] Tsutomu Suzuki,[§] and John J. Perona*[,†,‡]

[†]Department of Chemistry, Portland State University, 1825 SW Broadway, Portland Oregon 97209, United States

[‡]Department of Biochemistry & Molecular Biology, Oregon Health & Sciences University, 3181 SW Sam Jackson Park Road, Portland Oregon 97209, United States

[§]Department of Chemistry and Biotechnology, Graduate School of Engineering, The University of Tokyo, 7-3-1 Hongo, Bunkyo-ku, Tokyo, 113-8656, Japan

S *Supporting Information*

ABSTRACT: Folding dynamics are ubiquitously involved in controlling the multivariate functions of RNAs. While the high thermodynamic stabilities of some RNAs favor purely native states at equilibrium, it is unclear whether weakly stable RNAs exist in random, partially folded states or sample well-defined, globally folded conformations. Using a folding assay that precisely tracks the formation of native aminoacylable tRNA, we show that the folding of a weakly stable human mitochondrial (hmt) leucine tRNA is hierarchical with a distinct kinetic folding intermediate. The stabilities of the native and intermediate conformers are separated by only about 1.2 kcal/mol, and the species are readily interconvertible. Comparison of folding dynamics between unmodified and fully modified tRNAs reveals that post-transcriptional modifications produce a more constrained native structure that does not sample intermediate conformations. These structural dynamics may thus be crucial for recognition by some modifying enzymes *in vivo*, especially those targeting the globular core region, by allowing access to pretransition state conformers. Reduced conformational sampling of the native, modified tRNAs could then permit improved performance in downstream processes of translation. More generally, weak stabilities of small RNAs that fold in the absence of chaperone proteins may facilitate conformational switching that is central to biological function.

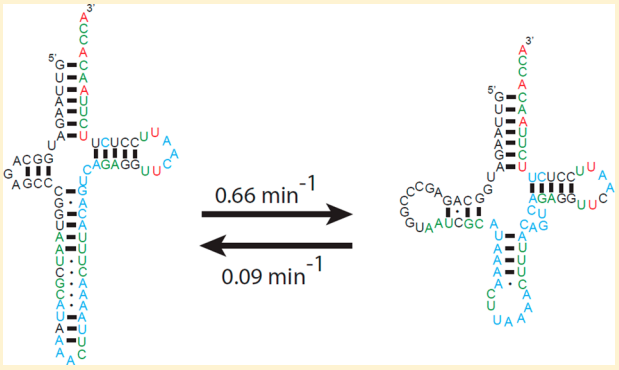

The structural dynamics of RNAs play critical roles in pre-mRNA splicing,[1] ribosome assembly,[2] virus replication,[3] and gene regulation by metabolite-responsive riboswitches.[4] Although proteins may bind either transiently or tightly to facilitate these RNA structural transitions,[5,6] the ability to traverse varied conformational space is a fundamental property of RNAs.[7,8] Indeed, *in vitro* folding studies have demonstrated that RNAs in general fold through rugged folding landscapes with several energetic minima, implying the existence of distinct stable conformations during folding. Exchange among these conformations can be slow or limited, however, because of strong local base-pairing and stacking interactions present in each state.[9]

Fundamental insight into RNA folding dynamics requires an understanding of both thermodynamic and kinetic aspects of the process. A key role is played by diffuse and site-specific Mg^{2+} ions.[10] For several RNAs, Mg^{2+}-induced folding is hierarchical with distinct folding intermediates, and the rate-limiting step occurs late in the folding pathway.[11] The magnitude of the energetic barrier between the late intermediate and final native states then determines the kinetics of folding. In the *Tetrahymena* self-splicing RNA, the rate by which a late intermediate is converted to the native state is decreased at high Mg^{2+} concentration, presumably because the intermediate is stabilized under these conditions.[12] Determining the stability of the native RNA relative to the last populated kinetic intermediate is a primary goal of RNA folding studies since this controls which species predominates at equilibrium.[11]

A common approach to determine the stability of structured RNAs is the monitoring of structure formation at specified Mg^{2+} concentrations, using biophysical methods such as gel shift, UV-absorbance or fluorescence. The Mg^{2+} dependencies are then used to calculate Hill coefficients, from which estimates of stability of the RNAs are obtained. However, Mg^{2+}-induced folding can yield a variety of different structural intermediates possessing similar free energies.[13,14] Thus, these methods cannot accurately determine the relative stabilities of native versus intermediate states for structured RNAs, without an implicit two state-assumption.[15,16] In contrast, by employing a combination of strategies, the native state of the catalytic domain of bacterial RNase P was found to be about 50-fold (2 kcal/mol) more stable

Received: October 24, 2013
Revised: February 7, 2014
Published: February 12, 2014

   dx.doi.org/10.1021/bi401449z | *Biochemistry* 2014, 53, 1456−1465

than a kinetic intermediate,[17] whereas that of the *Tetrahymena* group I ribozyme was 3.5 to 7 kcal/mol more stable.[18] Both of these large RNA intermediates also refold slowly to the native state, indicating the existence of kinetic barriers.[17,19,20] These barriers may also prevent unfolding of the native state to the intermediate in a simple two-step reaction model, where the states possess comparable stabilities.[21]

Small RNAs are known to form kinetically trapped intermediates during folding. Several misfold under low salt and low temperature conditions, and then readily convert to native forms when heated or when the ionic strength is increased.[22−24] For example, *E. coli* $tRNA^{Trp}$ and 5S rRNA exist in both active and inactive forms that require high activation energies for interconversion.[22,25−27] While no experimentally determined values for the relative stabilities of native versus intermediate states currently exist for these RNAs, it may be reasonable to assume that they populate the native states nearly exclusively if these states are highly stable. However, for RNAs that possess relatively weak global stabilities, it is unclear what native and non-native conformations are populated and how folding dynamics in turn affects function. The dynamic motions of small RNAs have been studied by a variety of methods;[28,29] for example, single-molecule fluorescence resonance energy transfer (smFRET) studies demonstrated that the hairpin, hammerhead, and *Tetrahymena* ribozymes each interconvert among different functional conformational states at equilibrium.[30−33] However, smFRET does not distinguish between native and non-native states of an RNA because their structural signatures can be highly similar.[20,34,35] Additionally, because the non-native states retain many native tertiary contacts, these methods require prior knowledge about the folding pathways to elucidate the conformational transitions that occur between the native and non-native states. A direct assay of the native state achieved by exploiting catalytic properties of the RNA alone, or a protein enzyme that acts upon it, is therefore desirable.

Previously, we developed such a strategy to accurately monitor the kinetics and thermodynamics of tRNA folding based on the ability of ^{32}P-labeled tRNAs to be aminoacylated.[36] We now apply this approach to probe the folding of a highly destabilized disease-relevant mitochondrial tRNA. Mitochondrial tRNAs are good models for studying the effects of weakly stable native structure on the functional properties of the molecule since many of them lack key conserved structural elements found in all canonical cytoplasmic and bacterial species. For example, most mitochondrial tRNAs do not possess one or more of the conserved nucleotides necessary to form tertiary contacts between the D- and T-loops in the globular hinge region of the molecule (Figure 1A). Some other mitochondrial species, including all the mammalian $tRNA^{Ser}$ acceptors, are missing large portions of the D-arm that appear necessary to the structural integrity of the tertiary core (Figure 1A).[37,38] The absence of these otherwise highly conserved structural features correlates with the general instability of mitochondrial tRNAs and may account for why none of these species has been successfully crystallized.

We show here that the native state stability of unmodified hmt $tRNA^{Leu}_{UAA}$ is only about 7.3-fold higher than that of a kinetic on-pathway, non-native intermediate. This intermediate is unstable and readily refolds to the native state, but because the native state is only marginally more stable than the intermediate, there is a small but consistent accumulation of intermediate at equilibrium. Strikingly, we show that the native state can also periodically unfold to form the intermediate state even at high Mg^{2+} concentrations. This creates a steady exchange of conformations where native and intermediate states are constantly sampled. In contrast to the unmodified tRNA, the dynamic exchange of conformations in the fully modified form of bovine mitochondrial (bmt) $tRNA^{Leu}$ is restricted. Our model suggests that the dynamicity to populate native and non-native species during folding is an important feature of weakly stable RNAs.

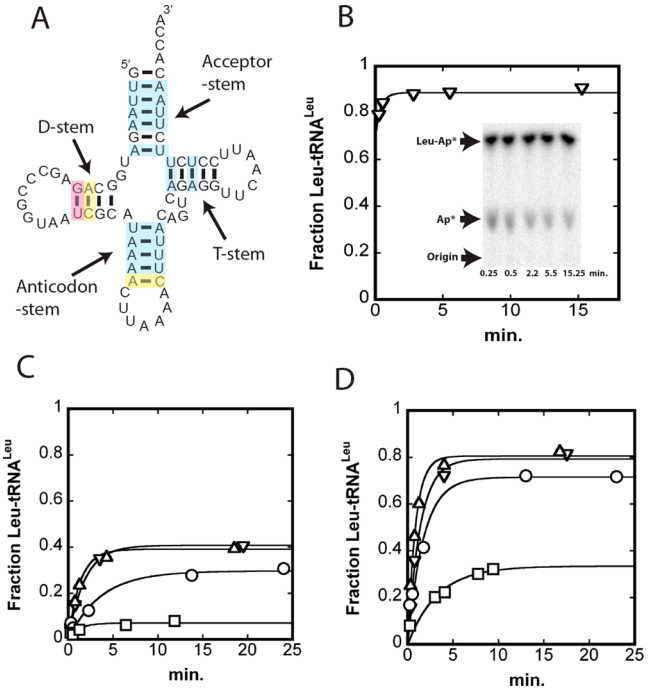

Figure 1. Aminoacylation of hmt $tRNA^{Leu}_{UAA}$. (A) Secondary structure of Hmt $tRNA^{Leu}_{UAA}$. A−U pairs are highlighted in blue, A−C mismatches in yellow, and the G−U pair in pink. (B) Hmt $tRNA^{Leu}_{UAA}$ was incubated in 20 mM Mg^{2+}, 2.5 mM ATP, and 10 mM leucine for 5 min. The aminoacylation reaction was then initiated by the addition of 5 μM LARS2. The inset shows a TLC image of the reaction following P1 nuclease digestion of the tRNA to nucleotides and separation; Leu-Ap* and Ap* represent leucylated and nonleucylated $tRNA^{Leu}_{UAA}$, respectively. These spots were quantitated, and the fractions of leucylated tRNAs were plotted over time to determine the maximum plateau value for aminoacylation at 93% (∇). A small fraction (about 5−10%) cannot be aminoacylated, most likely because of 3′-end heterogeneity and/or damage during the synthesis and labeling steps. (C) tRNA was first heat-denatured and then slow cooled to 21 °C; (D) tRNA was folded at 21 °C without heat-denaturation. Reactions in C and D were performed in the presence of 10 mM $Mg(CH_3COO)_2$ followed by the addition of 500 nM LARS2. Data depicted in panels C and D are derived from aminoacylation reactions performed at 15 °C (∇), 21 °C (Δ), 37 °C (○), and 45 °C (□). The highest plateau levels were obtained when the tRNA was both folded and aminoacylated at 21 °C. These experiments demonstrate that conventional refolding by heat-denaturation followed by slow cooling or aminoacylation at 37 °C or higher each give low aminoacylation plateau levels.

EXPERIMENTAL PROCEDURES

Hmt and bmt mitochondrial $tRNA^{Leu}_{UAA}$ were prepared by *in vitro* transcription. *In vivo*, post-transcriptionally modified bmt $tRNA^{Leu}$ was isolated from fresh bovine liver as described previously.[39]

LARS2 Purification. LARS2 was overexpressed in *E. coli* and purified as described previously.[40] The vector was transformed into Rosetta 2(DE3)pLysS competent cells (Novagen). The overnight culture was added to 1 L of LB media in the presence of

dx.doi.org/10.1021/bi401449z | *Biochemistry* 2014, 53, 1456−1465

35 μg/mL chloramphenicol and 34 μg/mL kanamycin. After the culture was grown at 37 °C to A_{600} of 0.8, expression was induced with 1 mM IPTG, and cells were then allowed to grow overnight at 15 °C. The cells from 1 L of saturated culture were centrifuged and resuspended in 35 mL of lysis buffer containing 20 mM sodium Hepes (pH 7.2) and 500 mM NaCl, followed by the addition of 150 μg of DNase I, 50 mg of lysozyme, and one pellet protease inhibitor [Complete Mini, ethylenediaminetetraacetic acid (EDTA)-free protease inhibitor cocktail tablets, Roche Diagnostics, GmbH, Germany]. The cells were sonicated for 15 min with an alternating 10 s pulse on/pulse off mode. The cell-free lysate was then centrifuged at 16,000 rpm for 45 min, and the supernatant was applied to a 2 mL Ni-NTA matrix PerfectPro Ni-NTA Agarose (5 PRIME) column pre-equilibrated in lysis buffer (20 mM sodium Hepes (pH 7.2), 500 mM NaCl, 10 mM imidazole, and 5 mM β-mercaptoethanol). The column was then washed sequentially with 30 column volumes of lysis buffer, 10 column volumes of buffer containing 20 mM imidazole, and finally with 2 column volumes of buffer containing 30 mM imidazole. Pure LARS2 was then eluted using a 250 mM imidazole. The protein was dialyzed against and stored in a buffer containing 25 mM Hepes-KOH (pH 7.2), 150 mM KCl, 5 mM β-mercaptoethanol, 0.2 mM EDTA, and 50% glycerol.

Purification and 3′-End Repair of Bovine Mitochondrial tRNA$^{Leu}_{UAA}$. *In vivo*, fully post-transcriptionally modified bovine mitochondrial tRNA$^{Leu}_{UAA}$ was isolated from fresh bovine liver as described previously.[39] The isolated tRNA possessed a truncated 3′-terminus possessing a cyclic phosphate (3′ CC > p), which was hydrolyzed by treatment with 0.1 M HCl for 3 h on ice. The acid-treated tRNA was then recovered by ethanol precipitation. Next, the tRNA was denatured by heating at 70 °C for 7 min and annealed at room temperature in a buffer containing 50 mM HEPES-KOH (pH 7.5) and 10 mM $MgCl_2$. After the addition of 5 mM DTT, the 3′-end of tRNA was dephosphorylated by the action of the 3′-phosphatase activity in T4 polynucleotide kinase (30 U/1 OD unit of tRNA, Toyobo). The 3′-end of the tRNA was then repaired with *E. coli* tRNA nucleotidyltransferase (5 μg/1 OD unit of tRNA) in a reaction consisting of 33.4 mM HEPES-KOH (pH 7.5), 100 mM KCl, 6.6 mM $MgCl_2$, 1.67 mM DTT, 1 mM ATP, and 1 mM CTP.[41] The repaired tRNA was extracted with Tripure Isolation Reagent (Roche) as instructed by the manufacturer and gel-purified on a 10% polyacrylamide gel containing 7 M urea. Finally, the tRNA was desalted by drop dialysis with MF-membrane filters (Millipore, 0.025 μm VSWP membrane). To check the quality of the 3′-terminus, the purified tRNA was digested by Interferase-MazF (TaKaRa) and subjected to liquid chromatography−mass spectrometry to observe the 3′-terminal fragments,[42] confirming that the 3′-terminus of the tRNA was fully repaired.

Activity Assay to Probe Equilibrium and Kinetics of Folding/Unfolding of tRNA$^{Leu}_{UAA}$. ^{32}P-labeled tRNA^{Leu} species with the label located at the 3′-internucleotide linkage were prepared as described previously for the transcript of *E.coli* tRNA^{Gln}.[43] All aminoacylation reactions were performed in the presence of 100 mM Na-Hepes (pH 7.0), 5 mM DTT, 10 mM leucine, 2.5 mM ATP-$Mg(CH_3COO)_2$, and the specified concentration of $Mg(CH_3COO)_2$. For equilibrium reactions, tRNA$^{Leu}_{UAA}$ was preincubated with Mg^{2+} (or Mg^{2+} and EDTA) for 30 min and the reaction initiated by the addition of LARS2. For monitoring rate-limited folding to the native state, tRNA$^{Leu}_{UAA}$ was preincubated in the absence of Mg^{2+} ions, and the reaction was initiated with the simultaneous addition of LARS2 and Mg^{2+}. For monitoring the unfolding reaction, a two-stage unfolding and aminoacylation reaction was set up. In the first stage, unfolding of tRNA^{Leu} was initated by the addition of EDTA to Mg^{2+}-preincubated tRNA^{Leu}; in the second stage, aliquots from this mixture were aminoacylated with the addition of LARS2 for 15 s. Reactions were quenched in 400 mM sodium acetate (pH 5.2) with 0.1% SDS, followed by the addition of P1 nuclease to 0.1 mg/mL and incubation for 10 min. Aliquots were spotted on previously water run and dried polyethyleneimine-cellulose thin-layer chromatography plates (Sigma). The plates were developed in 100 mM ammonium acetate and 5% (v/v) acetic acid, dried, and exposed to phosphorimaging screens overnight. Spots corresponding to [^{32}P]-labeled Leu-AMP and AMP were quantitated with ImageQuant (version 5.2), and the data were plotted in Kaleidagraph (version 4.03). All experiments were repeated at least twice, and the error rates are <10%.

SHAPE Analysis of Transcript hmt tRNA^{Leu}. SHAPE analysis footprinting experiments were conducted as described previously.[44] *N*-Methylisatoic anhydride (NMIA) was purchased from Sigma. A final concentration of 10 mM NMIA, which produces single-hit conditions as judged by the observation of full-length bands, was incubated with the tRNA construct at 30 °C for 1 h before ethanol precipitation and primer extension as described.[44] 1M7 analysis was performed similarly. DNA for *in vitro* transcription containing a T7 RNA polymerase binding site, 5′ linker, tRNA$^{Leu}_{UAA}$, 3′-linker, and reverse transcriptase binding site, in that order, was constructed using an Assembly PCR oligo maker.[45] Recursive gene synthesis was performed employing VENT DNA polymerase.[46] RNA was then prepared using *in vitro* transcription and gel purification.

RESULTS

To study the structural dynamics of a weakly stable RNA in detail, we selected the hmt tRNA$^{Leu}_{UAA}$ species that has previously been examined by structure probing and amino-acylation experiments.[47,48] This isoacceptor is one of the few mitochondrial tRNAs in humans possessing all of the conserved elements required for canonical tRNA tertiary folding (Figure 1A).[49] However, the unmodified transcript nonetheless does not adopt a canonical L-shaped structure at 37 °C and 12 mM Mg^{2+},[47] perhaps owing to the presence of a high proportion of A−U base pairs and a few A−C mismatches in the helical stem regions (Figure 1A). Footprinting experiments showed that under these conditions the acceptor and T stems are fully formed, but the D and anticodon stems comprising the vertical arm were unstructured. Despite this, the tRNA remained aminoacylable at levels up to 75%.[47,48] These findings suggested two alternative possibilities for the aminoacylation mechanism: (i) 75% of the partially structured transcript tRNA adopts the native and functional structure upon binding to leucyl-tRNA synthetase (LARS2) so that the enzyme functions as a folding chaperone; (ii) 75% of transcript tRNA is dynamic, such that unstructured tRNA transiently populates a canonical native structure that is then captured and aminoacylated by LARS2.

Optimal Folding and Aminoacylation of the hmt tRNA^{Leu} Unmodified Transcript. To address the folding dynamics of tRNA^{Leu}, we employed a sensitive assay that accurately distinguishes the native aminoacylable form of the tRNA from all other conformers.[36,50] The hmt tRNA^{Leu} transcript was ^{32}P-labeled at the 3′-internucleotide linkage as described previously[36,51] and then allowed to fold by incubation at 21 °C with the further addition of 20 mM Mg^{2+}(acetate). The capacity of the tRNA to serve as a substrate for aminoacylation by LARS2 was then evaluated at 21 °C, in the presence of 2.5 mM

ATP and 10 mM leucine (Leu) (Figure 1B). These optimized reaction conditions permit maximum aminoacylation plateau levels of 90−95%, higher than previously reported for any organellar tRNA transcript.[47] Further, neither the rate nor amplitude of aminoacylation was affected by preincubation of LARS2 with tRNA, suggesting that the enzyme does not function as a folding chaperone. These optimized folding conditions allow accurate determination of kinetic and thermodynamic parameters for tRNA folding, as described below. More conventional refolding protocols involving heat-denaturation and annealing steps, higher temperatures in aminoacylation, or use of chloride as the counterion gave lower aminoacylation plateau levels (Figure S1, Supporting Information), perhaps in part because of structural destabilization at high temperatures (Figures 1C,D and S2 (Supporting Information)). It is also known that acetate anions are generally less inhibitory to protein−RNA interactions as compared with chloride.[52]

Stability of the hmt tRNA$^{Leu}_{UAA}$ Unmodified Transcript. To evaluate the stability of hmt tRNA^{Leu}, we monitored the equilibrium fraction of native tRNA at varying Mg^{2+} ion concentrations under our optimized solution conditions (Figure 2A). Control experiments established that incubation of the

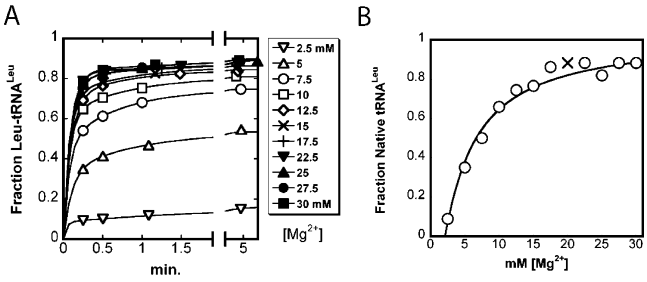

Figure 2. Mg^{2+}-dependent folding of the unmodified hmt tRNA$^{Leu}_{UAA}$ transcript. (A) Results of leucylation reactions performed at different concentrations of Mg^{2+} (as indicated on the right panel). The tRNA was preincubated in 2.5 mM ATP, 10 mM Leu, and the indicated concentrations of Mg^{2+} for 30 min before initiating the reaction with the addition of 5 μM LARS2 at 21 °C. The maximum aminoacylable fraction is 94%, and the maximum burst amplitude is 0.83. Because a small fraction, here 6%, represents damaged and nonaminoacylable tRNA, the true fraction of native tRNA at equilibrium is 0.88 after normalization. (B) Plot of the normalized burst amplitudes from panel A against Mg^{2+} concentration, giving $Mg_{1/2}$ of 6.55 mM. This represents the concentration at which half the hmt tRNA$^{Leu}_{UAA}$ is in the native state. The data point X represents normalized burst amplitude from the plot in Figure 1B.

tRNA for 30 min sufficed to reach equilibrium (data not shown). We then performed aminoacylation reactions on the pre-equilibrated mixture. At all Mg^{2+} concentrations, we observed biphasic kinetics with a rapid initial phase of aminoacylation followed by a slower phase (Figure 2A). In accordance with our detailed folding studies of archaeal tRNA^{Gln},[36] in which identical biphasic behavior was observed, we infer that the fast phase represents aminoacylation of already-folded species, while the slow phase represents aminoacylation of species that fold to the functional, aminoacylable state after the enzyme is added. The slow phases at lower Mg^{2+} concentrations (below 20 mM) exhibit lower plateaus than the maximum value observed at and above 20 mM Mg^{2+}. This indicates that at equilibrium larger fractions of tRNA do not fold to the native state at lower Mg^{2+} concentrations. Below we demonstrate that LARS2 is able to fully aminoacylate modified tRNA at low Mg^{2+}; thus, the lower plateau values do not represent enzyme inactivation under these conditions. At the higher Mg^{2+} concentrations, the maximum aminoacylable fraction is 94%, and the maximum burst amplitude is 0.83. Because a small fraction, approximately 6%, represents damaged and nonaminoacylable tRNA, the true fraction of native tRNA represented in the burst amplitude is 0.88 ± 0.01 after normalization.

Two sets of experiments were performed to determine if the high and stable maximum normalized burst amplitude of 0.88 ± 0.01 at 20 mM Mg^{2+} and higher represents the true equilibrium for the native state (Figure 3). We performed aminoacylation reactions by first incubating tRNA^{Leu} in the presence of 20 mM Mg^{2+} for 20 min and then adding varying concentrations of EDTA, an agent that chelates divalent metal ions. If the burst amplitudes indeed represent equilibrium fractions of native species, then we would expect to observe a decrease in burst amplitudes as EDTA concentrations are increased. In contrast, if bursts arise from a kinetic effect, then EDTA concentrations should have little or no influence on the amplitudes while perhaps affecting the rate of the slow phase. The data demonstrate that a decrease in burst amplitudes is indeed observed upon addition of EDTA, without any effect on the slow phase rate (Figure 3A). Thus, the amplitudes represent native fractions at equilibrium. The plot of burst amplitudes against Mg^{2+} concentrations shows that tRNA^{Leu} requires a very high concentration of Mg^{2+} ions ($Mg_{1/2}$ = 6.55 mM) to fold to the native state (Figure 2B; a small fraction of Mg^{2+} may remain associated with acetate at high concentrations (>40 mM),[53] thereby slightly overestimating the $Mg_{1/2}$). These results are in striking contrast to those observed for several canonical *in vitro* transcribed tRNAs in which $Mg_{1/2}$ was found to be 0.02−1 mM.[54,55] Thus, consistent with previous findings, these results suggest that the hmt tRNA^{Leu} transcript is highly destabilized compared to canonical tRNAs, despite its conventional cloverleaf secondary structure.

In the second set of experiments, we preincubated hmt tRNA$^{Leu}_{UAA}$ in K^+-Hepes buffer before simultaneously adding Mg^{2+} ions and LARS2, to initiate folding and aminoacylation at the same time. These Mg^{2+}-jump experiments isolate a rate-limiting folding step: the biphasic plot (rapid phase of ∼15 min^{-1} followed by a slow phase of ∼0.75 min^{-1}) (Figures 2A and 3A,C), is replaced by a uniphasic plot with a rate-constant of 0.7 min^{-1} (Figure 3B). This rate constant is about 15-fold lower than the aminoacylation rate constant for the fast phase under the same conditions (Figure 3C), suggesting that a large fraction of the tRNA either exists in non-native forms in the absence of Mg^{2+} ions or is converted to non-native forms immediately upon Mg^{2+} addition. The refolding data fits well to a single exponential function (Figure 3B), suggesting that the non-native species is either a unique misfolded form or multiple misfolded forms that behave kinetically as a single species. The non-native fractions depicted in Figure 2A represent this misfolded species because these fractions also fold to the native state with nearly the same slow (approximately 1 min^{-1}) rate constant (Figure 3B).

Because our results indicate that native and misfolded tRNAs are present as kinetically distinct species, we were able to quantitatively determine the extent to which the native conformer is stabilized over the misfolded conformer. Since the maximum fraction of native species that can be prefolded at equilibrium corresponds to a burst amplitude of 0.88, we calculate an equilibrium value of 7.3 for the native state over the misfolded state [$f = K/(1 + K)$] or a difference of 1.2 kcal/mol at 21 °C. Thus, at equilibrium, a fraction corresponding to 7.3/8.3

dx.doi.org/10.1021/bi401449z | *Biochemistry* 2014, 53, 1456−1465

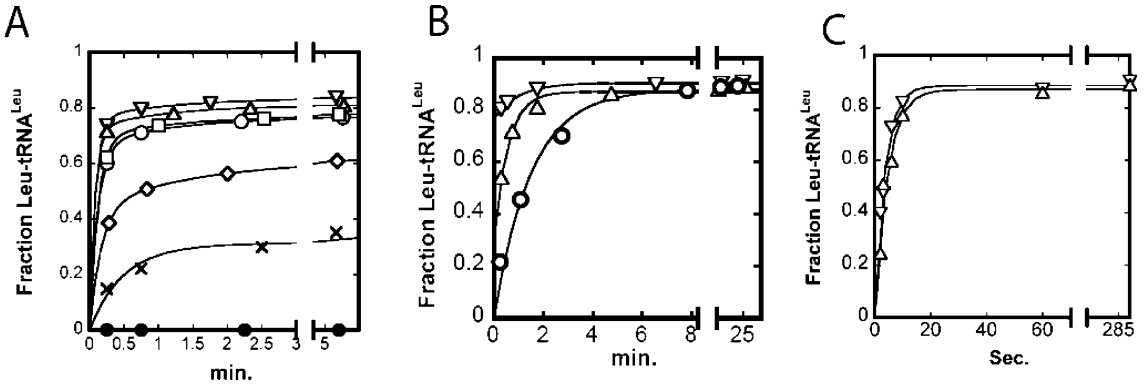

Figure 3. Interpretation of the burst amplitudes. (A) tRNA was preincubated in 20 mM Mg^{2+}, 2.5 mM ATP, 10 mM Leu, and EDTA concentrations of 0 mM (∇), 2.5 mM (Δ), 5 mM (○), 7.5 mM (□), 10 mM (◊), 12.5 mM (×), and 25 mM (●) for 30 min before initiating the reaction with the addition of 5 μM LARS2. The decrease in burst amplitudes reflects reduction in prefolded native tRNAs due to the decrease in free Mg^{2+} ion concentration as the concentration of EDTA is increased. (B) Transcript $tRNA^{Leu}_{UAA}$ was preincubated either in the absence (○) or presence of 3 mM Mg^{2+} (Δ) or 50 mM Mg^{2+} (∇), before simultaneously initiating the reaction with 5 μM LARS2 and readjusting the Mg^{2+} concentration to 50 mM for all three reactions. Rate constants were 0.7 min^{-1} (○) and 1.3 min^{-1} (Δ). Rate constants for fast (measured separately) and slow phases were 15 min^{-1} and 1 min^{-1} (∇), respectively. The normalized *Y*-intercepts corresponding to prefolded tRNA are 0.86 (∇) and 0.34 (Δ). (C) Rapid aminoacylation of preincubated $tRNA^{Leu}_{UAA}$. tRNA was preincubated in 20 mM $Mg(CH_3COO)_2$, 10 mM Leu, 2.5 mM ATP-$Mg(CH_3COO)_2$, 5 mM DTT, and 100 mM HEPES-KOH. The reactions were initiated by mixing with either 1 μM (Δ) or 5 μM LARS2 (∇) using rapid quenching. k_{obs} were 0.22 s^{-1} (13.2 min^{-1}) or 0.27 s^{-1} (16.2 min^{-1}) for reactions at 1 μM and 5 μM enzyme, respectively.

(88%) is in the native state, and 1/8.3 (12%) is misfolded. We previously used the same strategy to obtain an equilibrium value of 2.5 for the native state of an archaeal $tRNA^{Gln}$.[36]

Kinetic Intermediate during the Folding of Unmodified hmt $tRNA^{Leu}$. The observed slow folding behavior in Mg^{2+}-initiated reactions prompted us to further investigate the properties of the nonaminoacylable species. Specifically, we wished to address whether this species requires a large activation energy for folding to the functional conformation, as would be generally expected for a kinetic intermediate that must first undergo partial unfolding to access the native state. To examine this, we measured the dependence of folding on temperature (Figure 4A). The rate constant for tRNA refolding in Na^+-preincubated, Mg^{2+}-initiated reactions is indeed highly dependent on temperature: lower temperatures yielded lower rate constants for folding. The dependence of rate on temperature gave an apparent activation enthalpy of 32.8 kcal/mol (Figure S3, Supporting Information), consistent with disruption of 10−19 base-pairs.[36] In contrast, the rates for aminoacylation (fast phase) of prefolded $tRNA^{Leu}$ appear to be identical at all temperatures tested. Thus, the misfolded form is a kinetic on-pathway intermediate that requires disruption of the secondary/tertiary structure and partial unfolding to fold to the native state. Strikingly, the rate constants for the slow phases of aminoacylation of the prefolded tRNAs were comparable to the rate constants for refolding at all three temperatures tested (Figure 4, legend). These observations are highly consistent with the notion that the slow phase indeed represents the rate-limiting folding step from the intermediate to the native state.

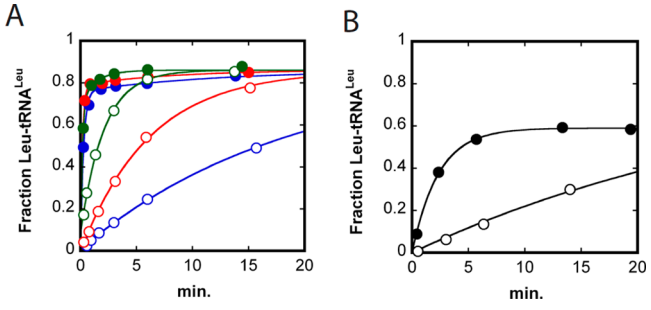

Figure 4. Dependence of folding on temperature and denaturant. (A) hmt transcript $tRNA^{Leu}_{UAA}$ was either preincubated in 100 mM Na^+-Hepes (open symbols) or prefolded in 100 mM Na^+-Hepes and 50 mM Mg^{2+} (solid symbols) at 10 °C (blue), 15 °C (red), or 21 °C (green) before initiating the reaction with the addition of 5 μM LARS2. Reactions preincubated in the absence of Mg^{2+} fit well to single exponential functions giving rate constants of 0.05 min^{-1}, 0.16 min^{-1}, and 0.5 min^{-1} at 10, 15, and 21 °C, respectively. The reactions preincubated in the presence of Mg^{2+} (solid symbols) were best fit to double exponential functions, with the rates of slow phases being 0.08 min^{-1}, 0.13 min^{-1}, and 0.7 min^{-1} at 10, 15, and 21 °C, respectively. (B) Hmt transcript $tRNA^{Leu}_{UAA}$ was allowed to refold at 10 °C as in panel A (○) or was preincubated in 1 M urea before initiating the reaction with LARS2 (●). k_{obs} derived from the data are 0.03 min^{-1} (○) and 0.43 min^{-1} (●).

We also performed a partial urea-denaturation experiment to determine if the kinetic intermediate unfolds by disruption of base-pairs and tertiary contacts.[11] We monitored the refolding of $tRNA^{Leu}$ at 10 °C as depicted in Figure 4A, except that the tRNA was preincubated in 1 M urea prior to aminoacylation. This low concentration was chosen based on previous studies on GlnRS that demonstrated only negligible denaturing effects of 1 M urea but required 18 h and much higher (>3 M) concentrations for substantial denaturation.[57] As shown in Figure 4B, we observed a 14-fold increase in the rate constant for refolding of tRNA under these conditions. This suggests that during the process of refolding of tRNA from the intermediate to the native state there is substantial disruption of secondary and/or tertiary contacts. Therefore, it seems clear that addition of urea accelerates refolding to the native state. Additionally, we observed that the plateau value in the presence of urea was reduced from 0.86 to 0.59, suggesting that either the denaturant also partially unfolds the native state under the solution conditions tested or that urea stabilizes a completely unfolded fraction that is unable to fold to the native state.

Dynamic Exchange of Conformations between Native and Intermediate States. The equilibrium value of 7.3 for the native state relative to the intermediate, together with an

dx.doi.org/10.1021/bi401449z | *Biochemistry* 2014, 53, 1456−1465

observed rate of refolding of 0.75 min^{-1} for conversion of the intermediate to the native conformation (Figure 2A, 3), allowed calculation of the individual forward and reverse rate constants as 0.66 min^{-1} and 0.09 min^{-1}, respectively. The data are consistent with a two-step model in which addition of Mg^{2+} ions results in formation of a kinetic intermediate, which then refolds to the native state. However, because the native state is only marginally more stable, and the kinetic barrier between states is low at 21 °C or higher, it appears possible that the native state also may unfold, albeit less frequently, to form the intermediate. This would generate a steady sampling of conformations at defined rates at equilibrium (Scheme 1). In a two-state model, the approach to

Scheme 1

equilibrium from native to intermediate should produce the same observed rate constant as that for folding of the intermediate to the native state (about ~0.75 min^{-1}).

To test this prediction, we directly monitored unfolding of the native state by taking advantage of the fact that addition of EDTA reduces the free Mg^{2+} ion concentration but does not affect the rates of the folding and unfolding transitions. Thus, we prefolded the tRNA at a concentration of 20 mM Mg^{2+} and then titrated EDTA into this prefolded mixture at 21 °C (Figure 5A). At each

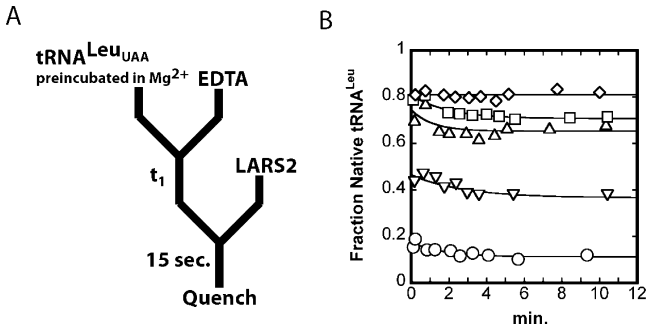

Figure 5. Monitoring unfolding of Hmt $tRNA^{Leu}_{UAA}$. (A) Scheme for unfolding experiment. (B) Unfolding was initiated by the addition of 2.5 mM (◊), 5 mM (□), 7.5 mM (Δ), 10 mM (∇), and 12.5 mM (○) EDTA to $tRNA^{Leu}_{UAA}$ preincubated in the presence of 20 mM Mg^{2+} for 30 min. Aliquots from this folding reaction were added to LARS2 (5 μM) in separate tubes and incubated for exactly 15 s before quenching with 1% SDS, followed by P1 nuclease digestion. The rate constants were about 1 min^{-1} at all concentrations of Mg^{2+}.

concentration of EDTA tested, we indeed observed small but consistent decreases in the fraction of native state that is populated over time, following EDTA addition. In each case, the data fit well to a single exponential function yielding a rate constant of about 1 min^{-1} (Figure 5B). Unfolding was observed at 5−12.5 mM EDTA concentrations; at 2.5 mM EDTA, the equilibrium is not perturbed, and thus no unfolding was observed. Thus, the native and intermediate states are engaged in a dynamic exchange of conformations with the equilibrium slightly favoring the native state over the intermediate.

To provide a structural basis for the observed folding dynamics, we next performed selective 2′-hydroxyl acylation analyzed by primer extension (SHAPE) experiments, using *N*-methylisatoic anhydride (NMIA) as a probe (Figure 6). At 30 °C and 40 mM $MgCl_2$, we observed extensive reactivities of the anticodon stem and variable loops. Absolute reactivities at these nucleotides are above 16% at both bases of a pair and thus are more flexible (Figure 6). We also performed SHAPE experiments in the presence of the reagent 1M7, which is not influenced by the presence of high $MgCl_2$ (>40 mM); these reactions were performed at 0, 12, and 50 mM $MgCl_2$ (Figure S4, Supporting Information). On the basis of the presumption that base-pairs are stabilized at higher concentrations of Mg^{2+}, we inferred that bases showing decreased reactivity as the Mg^{2+} concentration was increased are unpaired at the lower concentrations. The structural model obtained from this analysis shows an unpaired anticodon stem and variable loop region, whereas other parts of the tRNA appear to be well formed. These data are consistent with earlier findings for this tRNA, in which the anticodon and D-stems showed extensive reactivities in nuclease footprinting assays.[47] Thus, the structural dynamics are confined to the tRNA vertical arm. Analysis of this tRNA using the secondary structure prediction algorithm MC-fold suggested that an elongated structure containing an intact acceptor stem and T-stem, but mispaired D and anticodon stems, is most stable. Predicted suboptimal structures also exhibited these characteristics (Figure S5, Supporting Information). Thus, we propose that the kinetic intermediate features an intact acceptor stem and T-stem, and non-native secondary structure in other parts of the molecule (Figure 7).

Post-Transcriptional Modifications Stabilize the Native State of Bovine Mitochondrial $tRNA^{Leu}$. The influence of post-transcriptional modifications on dynamics was investigated for the related bmt $tRNA^{Leu}$. This tRNA is structurally very similar to hmt $tRNA^{Leu}$ and possesses an identical set of modifications in the globular core domain (Figure S6, Supporting Information). The human enzyme LARS2 efficiently aminoacylates both the unmodified transcript and the fully modified bmt $tRNA^{Leu}$ isolated from bovine tissue (Figure 8). The unmodified bmt $tRNA^{Leu}_{UAA}$ transcript exhibited dynamic folding behavior similar to hmt $tRNA^{Leu}_{UAA}$, with a persistent slow phase of refolding at equilibrium and in Mg^{2+}-jump experiments (Figure 8A,B). Thus, the folding behavior of the bmt tRNA is also consistent with a model of kinetic intermediates refolding to the native state.

We compared the Mg^{2+} ion dependence of folding between modified and unmodified bmt $tRNA^{Leu}$. We observed that *in vivo* tRNA prepared in the absence of Mg^{2+} is partially folded in the absence of externally added Mg^{2+} (Figure 8C). In contrast to the unmodified tRNA, the time courses for folding of modified tRNA at all Mg^{2+} concentrations showed no slow phases within the 10−20 s time limit of manual pipetting. These results suggest that the post-transcriptionally modified tRNA does not engage in slow exchange of conformations on a time scale comparable to that of the unmodified transcript. Further, the modified tRNA requires much less Mg^{2+} for folding to the native state at equilibrium ($Mg_{1/2}$ of 0.59 versus 2.23 mM) (Figure 8D). This effect is clearly attributable to the increased stability afforded by the presence of the post-transcriptional modifications.

■ DISCUSSION

The structural dynamics of weakly stable RNAs and the role of intermediates during folding have not previously been well-documented. Here, we exploited the known weak local stability of the anticodon arm of unmodified hmt $tRNA^{Leu}_{UAA}$ (Figure 1A) to address these issues. Using a sensitive aminoacylation-based folding assay, we show that the local structural fragility

dx.doi.org/10.1021/bi401449z | *Biochemistry* 2014, 53, 1456−1465

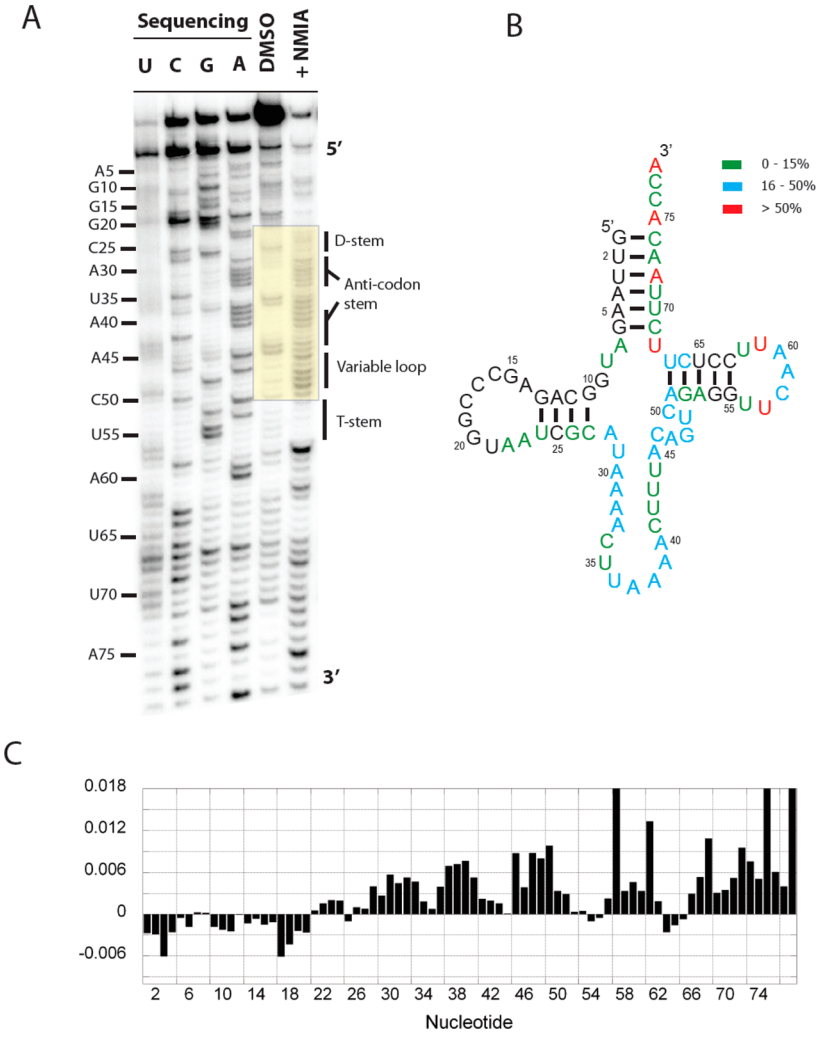

Figure 6. SHAPE footprinting with the sequencing lanes (U, C, G, and A) labeled at every 5 nucleotides. DMSO lane (solvent only) control lane and NMIA (SHAPE reagent) lanes are also shown. The U, C, G, and A sequencing ladder lengths are exactly one nucleotide longer than the corresponding DMSO and +NMIA product lengths. (A) The experiment demonstrates extensive reactivities of the D-stem, anticodon stem, and variable loops of hmt $tRNA^{Leu}_{UAA}$ at 30 °C and 40 mM $MgCl_2$. (B) Proposed structural model based on the SHAPE experiments. Absolute SHAPE intensities were binned into 0−15%, 16−50%, and >50%, and corresponding nucleotides are color-coded. (C) Absolute SHAPE reactivities were calculated from subtracting the intensities in the DMSO lane from those in the +NMIA lane.

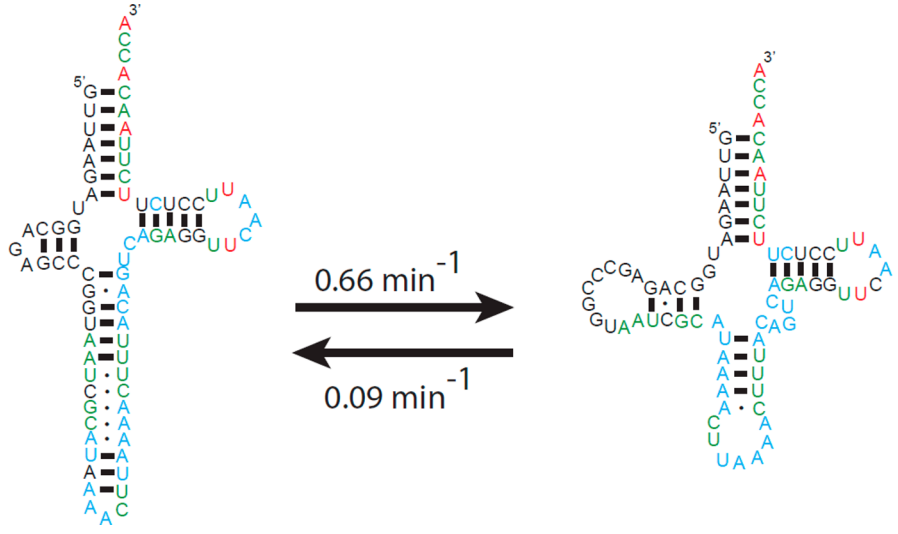

Figure 7. Proposed model for hmt $tRNA^{Leu}$ dynamics. Nucleotide residues are color-coded based on SHAPE intensities as described in Figure 6.

dx.doi.org/10.1021/bi401449z | *Biochemistry* 2014, 53, 1456−1465

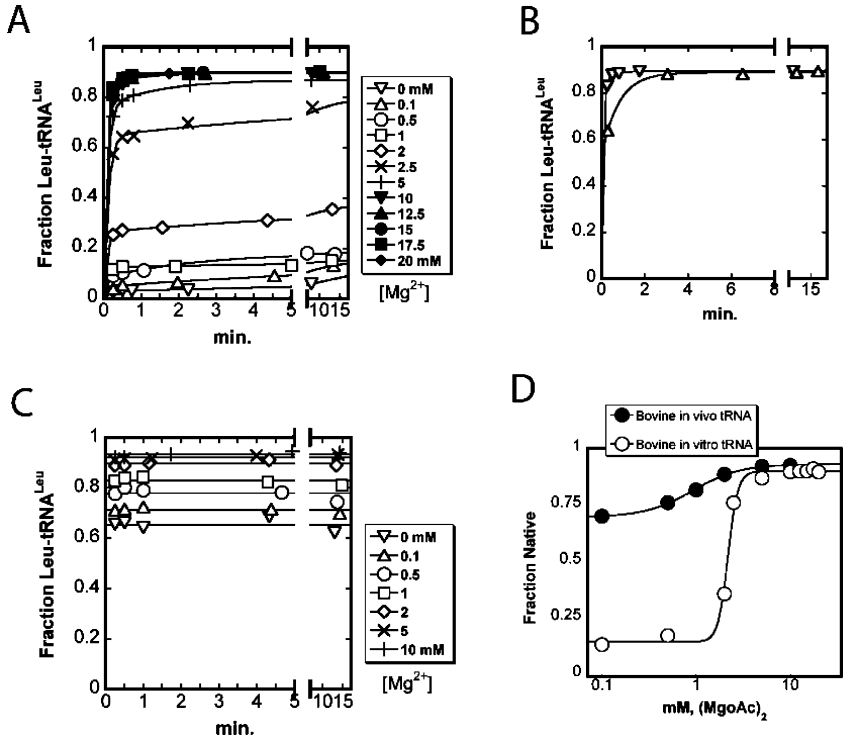

Figure 8. Effect of modifications on native state stability and dynamics of bmt tRNA^{Leu}. (A) Leucylation reactions of the bmt tRNA$^{Leu}_{UAA}$ transcript performed at different concentrations of Mg^{2+}. The tRNA was preincubated in 2.5 mM ATP, 10 mM Leu, and the indicated concentrations of Mg^{2+} for 30 min before initiating the reaction with the addition of 5 μM LARS2. (B) Leucylation reaction of bmt tRNA$^{Leu}_{UAA}$ transcript preincubated either in the absence or presence of 20 mM Mg^{2+}, before simultaneously initiating the reaction with 5 μM LARS2 and readjusting the Mg^{2+} concentration to 20 mM Mg^{2+}. Rate constants for the slow phases were 1.27 min^{-1} (Δ) and 1.42 min^{-1} (∇), and the Y-intercepts were 0.53 and 0.86, respectively. The rate constants for the fast phases were too fast to be measured by manual pipetting. (C) Leucylation reactions of modified bmt tRNA^{Leu} isolated from cells, performed as described for panel A. (D) Plot of the normalized fraction of the native state as a function of Mg^{2+} concentration. The half-maximum Mg^{2+} concentrations for folding to the native state ($Mg_{1/2}$) are 0.59 mM for modified tRNA and 2.23 mM for the unmodified transcript tRNA.

results in a highly destabilized global structure, as the tRNA requires a very high concentration of Mg^{2+} ions ($Mg_{1/2}$ = 6.55 mM) to fold to the native conformation. We then demonstrate that the degree of destabilization is such that the native state is only about 7.3-fold (1.16 kcal/mol) more stable than a kinetic intermediate. Thus, the unmodified hmt tRNA^{Leu} cannot populate the native state exclusively. Our results also suggest that the physiological temperature of 37 °C may be too high to stably populate native *in vitro* transcribed tRNAs for folding studies. Therefore, optimal temperature and solution conditions may have to be empirically determined for individual mitochondrial tRNAs as demonstrated in this study.

Since LARS2 does not influence either the thermodynamic equilibrium between native and intermediate, or the rate of folding, it appears unlikely that the enzyme functions as a chaperone. In the case of hmt tRNA^{Leu}, pathological disease mutations are located throughout the D and anticodon arms.[58,59] It is possible that the preponderance of disease mutations in these portions of the tRNA arises because the mutations further destabilize the already weakly stable native state, shifting the equilibrium to the misfolded intermediate. Mutations might also affect the folding dynamics such that both the native and intermediate are poorly populated, thereby reducing the ability of modification enzymes to recognize either form of the molecule. In fact, the most common disease-causing mutation, the A3243G alteration that is implicated in MELAS disease, results in the absence of a crucial taurine modification at position 34 without any change in other modifications, possibly because A3243G selectively alters the folding pathway.[60]

We also find that the kinetic barrier between the intermediate and the native state is sufficiently low that the two species can readily interconvert. The refolding of intermediate to the native state is much faster at higher temperature, as expected for a kinetically trapped species possessing non-native contacts. SHAPE analysis, structural predictions using MC-fold, and prior data[47] consistently demonstrate that the acceptor/T-stems of the unmodified tRNA are stable so that the destabilization is localized to the vertical anticodon arm. The non-native duplex structure predicted in the intermediate requires unwinding to allow for the formation of the D and anticodon stem structures in the native tRNA. This is consistent with the slow temperature-dependent refolding observed during conversion of the intermediate to the native state.

In general, *in vivo* folding of RNAs is faster than transcription;[61] therefore, a dynamic structure may prevent RNAs from becoming trapped in a local conformation. The sampling of conformations by unfolding to and refolding of a kinetic intermediate is likely *in vivo* because the dynamics we have observed occurs at physiological Mg^{2+} concentrations of 1−5 mM. Our results suggest that at very low Mg^{2+} concentrations only a fraction of the tRNA folds to the native state, while the remainder remains either unfolded or partially folded. Even the small fraction that folds to the native state at low Mg^{2+} levels shows sampling of conformations between native and the intermediate states. Thus, cells could modulate dynamics of tRNAs by altering concentrations of Mg^{2+} or possibly also of polyamines such as spermine.[62]

dx.doi.org/10.1021/bi401449z | *Biochemistry* 2014, 53, 1456−1465

As we have also demonstrated, post-transcriptional modifications can affect the equilibrium distribution of unfolded, partially folded, and native species in tRNA.[36,63] We suggest then that the recognition of bases and ribose sugars in the globular hinge domain of tRNA may depend upon an intrinsic dynamic instability of the tertiary structure in this region. For example, archaeosine tRNA-guanine transglycosylase (ArcTGT) converts G15 in the core region to the archaeosine precursor 7-cyano-7-deazaguanine (preQ0). The cocrystal structure of ArcTGT shows that the tRNA core region is completely disrupted, with the tRNA adopting an extended conformation when bound to the enzyme.[64] Dynamic unfolding and refolding of the unmodified tRNA could thus play a central role in the efficiency of the enzyme.

The finding that weakly stable RNAs can dynamically exchange between specific conformations may also have strong implications for functions of RNAs that follow a simple two-step folding−unfolding processes, including riboswitches. For example, the Trp terminator/antiterminator element contains multiple CUG triplets thought to destabilize the formation of stable duplexes and allow for efficient Trp-dependent switching from antiterminator to terminator structures.[65] Another example is translational frameshifting on the ribosome, in which control by RNA depends not only on the formation of a folded pseudoknot structure but also on partial unfolding of the pseudoknot to hairpins.[66] Thus, dynamic exchange by lowering of stabilities might play an important role in controlling the switch between two functional structures.

■ ASSOCIATED CONTENT

Supporting Information

Magnesium acetate gives higher plateau charging values for hmt $tRNA^{Leu}_{UAA}$ transcript compared to magnesium chloride; aminoacylation plateau value is low at higher temperature (>37°C) for hmt $tRNA^{Leu}$; log-linear plot of the rate constant against $1/T$ (K) for folding of the hmt $tRNA^{Leu}_{UAA}$ transcript; 1M7 SHAPE analysis at different Mg^{2+} concentrations; predicted optimal (upper left) and sub-optimal secondary structures of hmt $tRNA^{Leu}_{UAA}$ transcript tRNA; and predicted native secondary structures (based on comparative sequence analysis) of human and bovine transcript $tRNA^{Leu}_{UAA}$. This material is available free of charge via the Internet at http://pubs.acs.org.

■ AUTHOR INFORMATION

Corresponding Author

*Tel: 503-725-2426. E-mail: perona@pdx.edu.

Present Address

[‖]H.B.: Department of Cancer Biology, The Scripps Research Institute, Jupiter, Florida 33458.

Funding

This work was supported by a grant from the National Institutes of Health (GM 63713) to J.J.P.

Notes

The authors declare no competing financial interest.

■ ACKNOWLEDGMENTS

We thank Michael King (Thomas Jefferson University) for providing the LARS2 expression vector.

■ REFERENCES

(1) Will, C. L., and Luhrmann, R. (2011) Spliceosome structure and function. *Cold Spring Harb. Perspect. Biol.*, 3.

(2) Talkington, M. W., Siuzdak, G., and Williamson, J. R. (2005) An assembly landscape for the 30S ribosomal subunit. *Nature 438*, 628−632.

(3) Ke, A., Zhou, K., Ding, F., Cate, J. H., and Doudna, J. A. (2004) A conformational switch controls hepatitis delta virus ribozyme catalysis. *Nature 429*, 201−205.

(4) Haller, A., Souliere, M. F., and Micura, R. (2011) The dynamic nature of RNA as key to understanding riboswitch mechanisms. *Acc. Chem. Res. 44*, 1339−1348.

(5) Herschlag, D. (1995) RNA chaperones and the RNA folding problem. *J. Biol. Chem. 270*, 20871−20874.

(6) Pan, C., and Russell, R. (2010) Roles of DEAD-box proteins in RNA and RNP folding. *RNA Biol. 7*, 28−37.

(7) Le, S. Y., Zhang, K., and Maizel, J. V., Jr. (2002) RNA molecules with structure dependent functions are uniquely folded. *Nucleic Acids Res. 30*, 3574−3582.

(8) Adilakshmi, T., Ramaswamy, P., and Woodson, S. A. (2005) Protein-independent folding pathway of the 16S rRNA 5′ domain. *J. Mol. Biol. 351*, 508−519.

(9) Dethoff, E. A., Chugh, J., Mustoe, A. M., and Al-Hashimi, H. M. (2012) Functional complexity and regulation through RNA dynamics. *Nature 482*, 322−330.

(10) Grilley, D., Soto, A. M., and Draper, D. E. (2006) Mg2+-RNA interaction free energies and their relationship to the folding of RNA tertiary structures. *Proc. Natl. Acad. Sci. U.S.A. 103*, 14003−14008.

(11) Sosnick, T. R., and Pan, T. (2003) RNA folding: models and perspectives. *Curr. Opin. Struct. Biol. 13*, 309−316.

(12) Pan, J., Thirumalai, D., and Woodson, S. A. (1999) Magnesium-dependent folding of self-splicing RNA: exploring the link between cooperativity, thermodynamics, and kinetics. *Proc. Natl. Acad. Sci. U.S.A. 96*, 6149−6154.

(13) Celander, D. W., and Cech, T. R. (1991) Visualizing the higher order folding of a catalytic RNA molecule. *Science 251*, 401−407.

(14) Schroeder, S. J. (2009) Advances in RNA structure prediction from sequence: new tools for generating hypotheses about viral RNA structure-function relationships. *J. Virol. 83*, 6326−6334.

(15) Das, R., Travers, K. J., Bai, Y., and Herschlag, D. (2005) Determining the Mg2+ stoichiometry for folding an RNA metal ion core. *J. Am. Chem. Soc. 127*, 8272−8273.

(16) Leipply, D., and Draper, D. E. (2010) Dependence of RNA tertiary structural stability on Mg2+ concentration: interpretation of the Hill equation and coefficient. *Biochemistry 49*, 1843−1853.

(17) Fang, X. W., Golden, B. L., Littrell, K., Shelton, V., Thiyagarajan, P., Pan, T., and Sosnick, T. R. (2001) The thermodynamic origin of the stability of a thermophilic ribozyme. *Proc. Natl. Acad. Sci. U.S.A. 98*, 4355−4360.

(18) Johnson, T. H., Tijerina, P., Chadee, A. B., Herschlag, D., and Russell, R. (2005) Structural specificity conferred by a group I RNA peripheral element. *Proc. Natl. Acad. Sci. U.S.A. 102*, 10176−10181.

(19) Zarrinkar, P. P., Wang, J., and Williamson, J. R. (1996) Slow folding kinetics of RNase P RNA. *RNA 2*, 564−573.

(20) Russell, R., Das, R., Suh, H., Travers, K. J., Laederach, A., Engelhardt, M. A., and Herschlag, D. (2006) The paradoxical behavior of a highly structured misfolded intermediate in RNA folding. *J. Mol. Biol. 363*, 531−544.

(21) McCully, M. E., Beck, D. A., and Daggett, V. (2008) Microscopic reversibility of protein folding in molecular dynamics simulations of the engrailed homeodomain. *Biochemistry 47*, 7079−7089.

(22) Gartland, W. J., and Sueoka, N. (1966) Two interconvertible forms of tryptophanyl sRNA in *E. coli*. *Proc. Natl. Acad. Sci. U.S.A. 55*, 948−956.

(23) Cole, P. E., and Crothers, D. M. (1972) Conformational changes of transfer ribonucleic acid. Relaxation kinetics of the early melting transition of methionine transfer ribonucleic acid (*Escherichia coli*). *Biochemistry 11*, 4368−4374.

(24) Cole, P. E., Yang, S. K., and Crothers, D. M. (1972) Conformational changes of transfer ribonucleic acid. Equilibrium phase diagrams. *Biochemistry 11*, 4358−4368.

(25) Aubert, M., Scott, J. F., Reynier, M., and Monier, R. (1968) Rearrangement of the conformation of *Escherichia coli* 5S RNA. *Proc. Natl. Acad. Sci. U.S.A. 61*, 292−299.
(26) Weidner, H., and Crothers, D. M. (1977) Pathway-dependent refolding of *E. coli* 5S RNA. *Nucleic Acids Res. 4*, 3401−3414.
(27) Weidner, H., Yuan, R., and Crothers, D. M. (1977) Does 5S RNA function by a switch between two secondary structures? *Nature 266*, 193−194.
(28) Micura, R., and Hobartner, C. (2003) On secondary structure rearrangements and equilibria of small RNAs. *ChemBioChem 4*, 984−990.
(29) Al-Hashimi, H. M., and Walter, N. G. (2008) RNA dynamics: it is about time. *Curr. Opin. Struct. Biol. 18*, 321−329.
(30) Zhuang, X., Bartley, L. E., Babcock, H. P., Russell, R., Ha, T., Herschlag, D., and Chu, S. (2000) A single-molecule study of RNA catalysis and folding. *Science 288*, 2048−2051.
(31) Rueda, D., Wick, K., McDowell, S. E., and Walter, N. G. (2003) Diffusely bound Mg^{2+} ions slightly reorient stems I and II of the hammerhead ribozyme to increase the probability of formation of the catalytic core. *Biochemistry 42*, 9924−9936.
(32) McDowell, S. E., Jun, J. M., and Walter, N. G. (2010) Long-range tertiary interactions in single hammerhead ribozymes bias motional sampling toward catalytically active conformations. *RNA 16*, 2414−2426.
(33) Solomatin, S. V., Greenfeld, M., Chu, S., and Herschlag, D. (2010) Multiple native states reveal persistent ruggedness of an RNA folding landscape. *Nature 463*, 681−684.
(34) Wu, M., and Tinoco, I., Jr. (1998) RNA folding causes secondary structure rearrangement. *Proc. Natl. Acad. Sci. U.S.A. 95*, 11555−11560.
(35) Baird, N. J., Ludtke, S. J., Khant, H., Chiu, W., Pan, T., and Sosnick, T. R. (2010) Discrete structure of an RNA folding intermediate revealed by cryo-electron microscopy. *J. Am. Chem. Soc. 132*, 16352−16353.
(36) Bhaskaran, H., Rodriguez-Hernandez, A., and Perona, J. J. (2012) Kinetics of tRNA folding monitored by aminoacylation. *RNA 18*, 569−580.
(37) Kumazawa, Y., Yokogawa, T., Hasegawa, E., Miura, K., and Watanabe, K. (1989) The aminoacylation of structurally variant phenylalanine tRNAs from mitochondria and various nonmitochondrial sources by bovine mitochondrial phenylalanyl-tRNA synthetase. *J. Biol. Chem. 264*, 13005−13011.
(38) Helm, M., Brulé, H., Friede, D., Giegé, R., Pütz, D., and Florentz, C. (2000) Search for characteristic structural features of mammalian mitochondrial tRNAs. *RNA 6*, 1356−1379.
(39) Suzuki, T., and Suzuki, T. (2007) Chaplet column chromatography: isolation of a large set of individual RNAs in a single step. *Methods Enzymol. 425*, 231−239.
(40) Park, H., Davidson, E., and King, M. P. (2003) The pathogenic A3243G mutation in human mitochondrial tRNALeu(UUR) decreases the efficiency of aminoacylation. *Biochemistry 42*, 958−964.
(41) Tomari, Y., Suzuki, T., Watanabe, K., and Ueda, T. (2000) The role of tightly bound ATP in Escherichia coli tRNA nucleotidyltransferase. *Genes Cells 5*, 689−698.
(42) Suzuki, T., Ikeuchi, Y., Noma, A., and Sakaguchi, Y. (2007) Mass spectrometric identification and characterization of RNA-modifying enzymes. *Methods Enzymol. 425*, 211−229.
(43) Rodriguez-Hernandez, A., and Perona, J. J. (2011) Heat maps for intramolecular communication in an RNP enzyme encoding glutamine. *Structure 19*, 386−396.
(44) Wilkinson, K. A., Merino, E. J., and Weeks, K. M. (2006) Selective 2′-hydroxyl acylation analyzed by primer extension (SHAPE): quantitative RNA structure analysis at single nucleotide resolution. *Nat. Protoc. 1*, 1610−1616.
(45) Rydzanicz, R., Zhao, X. S., and Johnson, P. E. (2005) Assembly PCR oligo maker: a tool for designing oligodeoxynucleotides for constructing long DNA molecules for RNA production. *Nucleic Acids Res. 33*, W521−525.
(46) Bowman, J. C., Azizi, B., Lenz, T. K., Roy, P., and Williams, L. D. (2012) Preparation of long templates for RNA in vitro transcription by recursive PCR. *Methods Mol. Biol. 941*, 19−41.
(47) Sohm, B., Frugier, M., Brule, H., Olszak, K., Przykorska, A., and Florentz, C. (2003) Towards understanding human mitochondrial leucine aminoacylation identity. *J. Mol. Biol. 328*, 995−1010.
(48) Sohm, B., Sissler, M., Park, H., King, M. P., and Florentz, C. (2004) Recognition of human mitochondrial tRNALeu(UUR) by its cognate leucyl-tRNA synthetase. *J. Mol. Biol. 339*, 17−29.
(49) Giegé, R., Sissler, M., and Florentz, C. (1998) Universal rules and idiosyncratic features in tRNA identity. *Nucleic Acids Res. 26*, 5017−5035.
(50) Ledoux, S., and Uhlenbeck, O. C. (2008) [3′-32P]-labeling tRNA with nucleotidyltransferase for assaying aminoacylation and peptide bond formation. *Methods 44*, 74−80.
(51) Bhaskaran, H., and Perona, J. J. (2011) Two-step aminoacylation of tRNA without channeling in Archaea. *J. Mol. Biol. 411*, 854−869.
(52) Lorsch, J. R., and Herschlag, D. (1998) The DEAD box protein eIF4A. 1. A minimal kinetic and thermodynamic framework reveals coupled binding of RNA and nucleotide. *Biochemistry 37*, 2180−2193.
(53) Archer, D. W., and Monk, C. B. (1964) Ion-association constants of some acetates by pH (glass electrode) measurements. *J. Chem. Soc.*, 3117−3122.
(54) Serebrov, V., Vassilenko, K., Kholod, N., Gross, H. J., and Kisselev, L. (1998) Mg2+ binding and structural stability of mature and in vitro synthesized unmodified *Escherichia coli* $tRNA^{Phe}$. *Nucleic Acids Res. 26*, 2723−2728.
(55) Shelton, V. M., Sosnick, T. R., and Pan, T. (2001) Altering the intermediate in the equilibrium folding of unmodified yeast tRNAPhe with monovalent and divalent cations. *Biochemistry 40*, 3629−3638.
(56) Sinan, S., Yuan, X., and Russell, R. (2011) The Azoarcus group I intron ribozyme misfolds and is accelerated for refolding by ATP-dependent RNA chaperone proteins. *J. Biol. Chem. 286*, 37304−37312.
(57) Mandal, A. K., Samaddar, S., Banerjee, R., Lahiri, S., Bhattacharyya, A., and Roy, S. (2003) Glutamate counteracts the denaturing effect of urea through its effect on the denatured state. *J. Biol. Chem. 278*, 36077−36084.
(58) Levinger, L., Morl, M., and Florentz, C. (2004) Mitochondrial tRNA 3′ end metabolism and human disease. *Nucleic Acids Res. 32*, 5430−5441.
(59) Suzuki, T., and Nagao, A. (2011) Human mitochondrial tRNAs: biogenesis, function, structural aspects, and diseases. *Annu. Rev. Genet. 45*, 299−329.
(60) Kirino, Y., Yasukawa, T., Ohta, S., Akira, S., Ishihara, K., Watanabe, K., and Suzuki, T. (2004) Codon-specific translational defect caused by a wobble modification deficiency in mutant tRNA from a human mitochondrial disease. *Proc. Natl. Acad. Sci. U.S.A. 101*, 15070−15075.
(61) Pan, T., and Sosnick, T. (2006) RNA folding during transcription. *Annu. Rev. Biophys. Biomol. Struct. 35*, 161−175.
(62) Quigley, G. J., Teeter, M. M., and Rich, A. (1978) Structural analysis of spermine and magnesium ion binding to yeast phenylalanine transfer RNA. *Proc. Natl. Acad. Sci. U.S.A. 75*, 64−68.
(63) Helm, M., Brule, H., Degoul, F., Cepanec, C., Leroux, J. P., Giege, R., and Florentz, C. (1998) The presence of modified nucleotides is required for cloverleaf folding of a human mitochondrial tRNA. *Nucleic Acids Res. 26*, 1636−1643.
(64) Ishitani, R., Nureki, O., Nameki, N., Okada, N., Nishimura, S., and Yokoyama, S. (2003) Alternative tertiary structure of tRNA for recognition by a posttranscriptional modification enzyme. *Cell 113*, 383−394.
(65) Babitzke, P. (1997) Regulation of tryptophan biosynthesis: Trp-ing the TRAP or how Bacillus subtilis reinvented the wheel. *Mol. Microbiol. 26*, 1−9.
(66) Giedroc, D. P., Theimer, C. A., and Nixon, P. L. (2000) Structure, stability and function of RNA pseudoknots involved in stimulating ribosomal frameshifting. *J. Mol. Biol. 298*, 167−185.